Title: A Domain-Based Evolution Model for Red Sea: New Sea-Floor Spreading Evidence

Author information

Name: Farhoud, Khamis

Position: Study and Seismic Team Lead, Anton Oil, Majnoon Oil Field, Basra, Iraq

Email: kh_farhoud@hotmail.com

Phone No.: +201116055558

Name: El-Barkooky, Ahmed N.

Position: Professor in the Geology Department of Cairo University

Email: abarkook@cu.edu.eg

Status of this Manuscript: This is a non-peer-reviewed preprint submitted to EarthArXiv.

A Domain-Based Evolution Model for Red Sea: New Sea-Floor Spreading Evidence

Khamis Farhoud[1], Ahmed N El-Barkooky[2]

[1]Petroleum Engineering department, Anton Oil, Majnoon Oil Field, Basra, Iraq.
[2]Geology Department, Cairo University, Cairo, Egypt

Correspondence to: Khamis Farhoud (kh_farhoud@hotmail.com)

keywords: Red Sea, Seafloor Spreading, Magnetic Stripes, Structural Inheritance, Arabian-Nubian Shield

Abstract

The propagation of the Red Sea continental margin remains unevaluated. Despite the unanimous agreement that the southern Red Sea axial ridge valley is underlain by juvenile oceanic crust, there is a lack of such agreement for the central and northern Red Sea. Significant issues relating to Red Sea tectonics are whether the Arabian and Nubian plates have been completely separated (i.e., oceanic crust lies beneath the Red Sea from coast to coast) or if the oceanic crust is restricted to the Red Sea median valley. Here, we interpret a new spreading span of at least 12.5 Ma of magnetic anomaly stripes located in the Central Red Sea, which represent ancient seafloor spreading. We show that the Red Sea basement structure exhibits different fault trends, wherein the Red Sea crust is controlled by offshore inherited Precambrian suture zones. Both these infrastructure suture zones and the Dead Sea-Aqaba-transform faults control the Red Sea crustal evolution.

1. Introduction

Considerable research has focused on the Red Sea continental margin and its crustal evolutionary sequence. Modern observations of the transition from continental breakup to the initiation of seafloor spreading have galvanized plate tectonics research. This study addresses salient topics, including the boundary between oceanic and continental crust, the possible seaward continuation of onshore Proterozoic sutures, and the long-standing dichotomy between previous crustal models. By reconciling inconsistencies through an integrated dataset of magnetic, gravity, bathymetry, seismic, and surface geology (Fig.1a-e), we propose a domain-based model for Red Sea development.

1.1. Review of Evolutionary Models

1.1.1. Early Foundations

Positive gravity anomalies on the Red Sea shoreline (Fig.1a) were first observed by Von Triulzi (1898) and documented by pendulum observations (Vening Meinesz, 1934). Farquharson (1935) and Owen (1938) identified the axial trough as a belt of narrow, straight-sided troughs. This axial center was later interpreted as a large basic intrusion (Girdler, 1958), which Tazieff (1952) and Girdler and Harrison (1957) linked to the axial deep (Fig.1candd). This activity was potentially related to the 107 km displacement of Arabia relative to Sinai (Quennell, 1956, 1959; Carey, 1958). Subsequent work by Drake et al. (1959) and Girdler and Peter (1960) confirmed these trough deeps and identified reversely magnetized rocks in the Gulf of Aden.

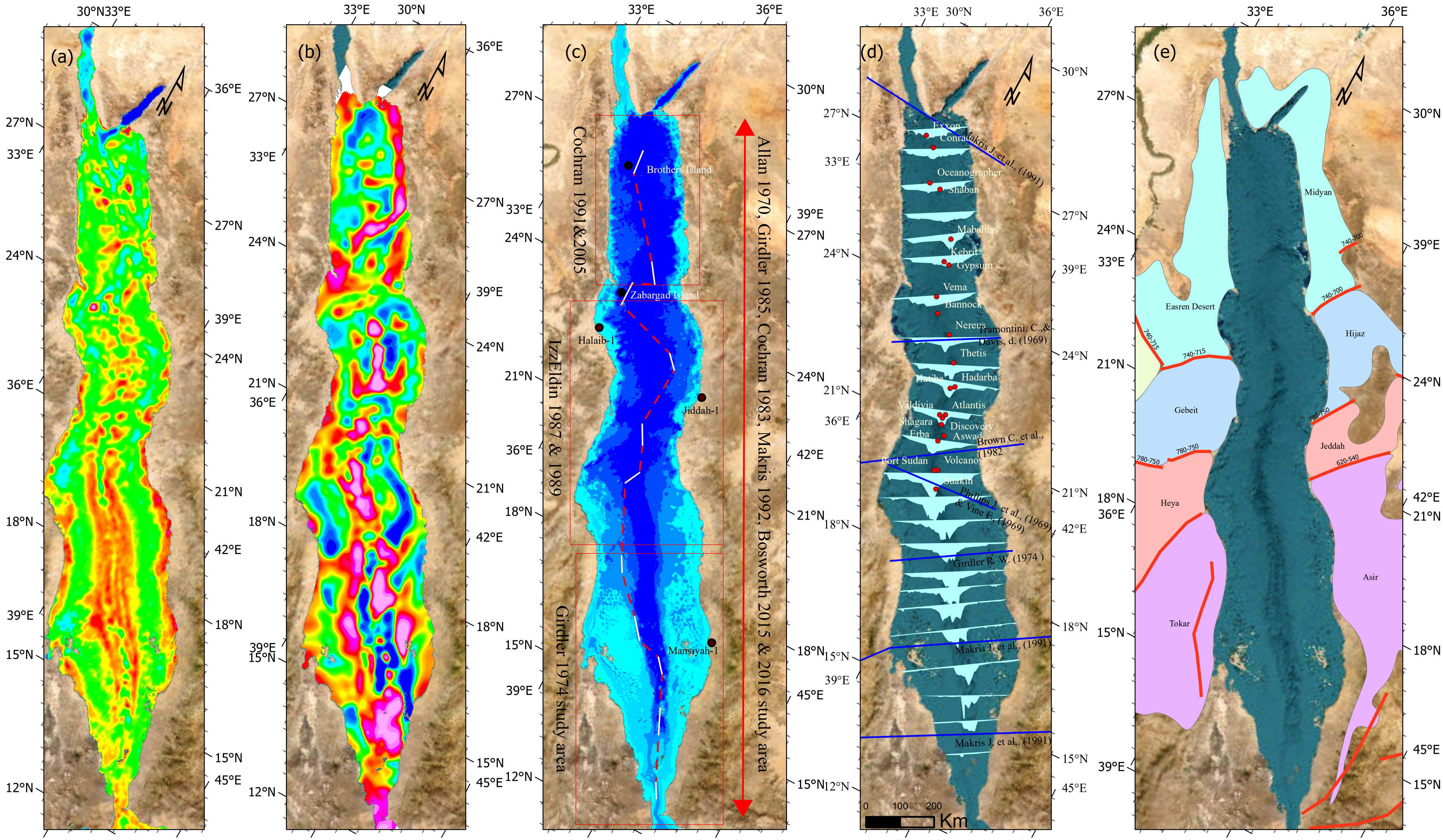

Figure 1: Regional Geophysical and Geological Datasets of the Red Sea. Maps (a) and (b) present the regional free-air gravity and magnetic intensity anomalies, respectively. Maps (c) and (d) illustrate the regional bathymetry. Map (e) provides a synthesized surface geological framework showing Precambrian suture zones (red lines) and crustal age domains/growth phases of the Arabian–Nubian Shield (modified after Fritz et al., 2013). In map (c), yellow solid lines indicate the locations of VEMA seismic refraction profiles (sourced from NCEI), and shaded boxes delineate previously studied geophysical focus areas. In map (d), red circles identify the locations of hydrothermal brine deeps, and solid lines indicate bathymetric profiles along the axial trough.

Data Sources: Potential field and bathymetric data were integrated from the World Digital Magnetic Anomaly Map (WDMAM v2.1), NOAA National Centers for Environmental Information (NCEI), and the UCSD Topographic/Bathymetric database. Map backgrounds are provided by Earthstar Geographics.

1.1.2. Development of the Seafloor Spreading Hypothesis

A pivotal discovery occurred when magnetic intensity lineations were first related to axial ridge valleys (Vine and Matthews, 1963), then Vine (1966) simulate magnetic profiles at Red Sea axial depression with spreading rate of 1 cm/yr for the past 5 Ma at latitude 16 and 20 degree. In current study, will use the same concept of Magnetic Polarity Stripes, where gravity and magnetic datasets (Fig.1a and b) are not merely used for structural mapping but serve as the primary diagnostic tools for crustal differentiation and delineate the boundaries of the Median Ridge Valley (MRV). Moreover, in the Red Sea, the axial trough exhibits seismic velocities between 6.7 and 7.3 km/s associated with distinct gravity and magnetic signatures (Drake and Girdler, 1964). While Wilson (1965) noted that spreading directions require the mapping of coeval transform faults, Allan (1966) provided a commendable amount of Red Sea regional data.

Refined seismic data subdivided the trough into axial and marginal zones (Knott et al., 1966). Girdler (1967) suggested the axial crust formed over the last 3-5 Ma, where the basement exhibits velocities of 6.4 km/s at depths of 3.3 to 3.7 km (Tramontini and Davies, 1969). Magnetic profiles at 19°N and 22°N suggested spreading over the last 2-4 Ma (Phillips et al., 1969), reconcilable with the 150 km northward movement of Arabia relative to Africa along the Abu Masorib-Duwi and Wadi Alhamd-Wadi Hafafit shear zones (Abdel-Gawad, 1969). Further mapping by Phillips and Ross (1970) and Allan (1970) delineated transform faults at 19°30'N.

1.1.3. Divergent Views on Crustal Composition

The nature of the northern Red Sea crust remains a central controversy. Girdler (1970) suggested it consists of extremely faulted continental crust (Fig. 1d shows the profiles locations of previous work), whereas McKenzie et al. (1970) argued the entire Red Sea is underlain by oceanic crust. Structural models emphasized the role of normal faulting (Lowell and Genik, 1972) and the presence of NW-trending en-echelon active volcanics (Stieltjes, 1973). Although basalt recovered at Site 226 showed MORB affinities (Stoffers and Ross, 1974), the identification of the "S" seismic reflector suggested spreading was post-Miocene (Roger et al., 1975). Conversely, Girdler and Styles (1974) identified 41 Ma oceanic crust, while Roeser (1975) identified 4-5 Ma anomalies, supported by gravity data at the Saudi margin (Gettings, 1977). An alternative school of thought suggesting the presence of sea floor spreading in the northern province (Girdler and Southren, 1987).

1.1.4. Regional Tectonics and Multi-Phase Evolution

Tectonic complexities include the Danakil microplate blocking the Afar depression (Le Pichon and Francheteau, 1978) and evidence for three phases of crustal development: 43-35.5 Ma, 23.5-16 Ma, and 4.5-0 Ma (Girdler et al., 1980) based on the LaBrecque et al. (1977) polarity scale. While a 1500 km gravity line suggested the entire sea is oceanic (Brown and Girdler, 1982) (Fig.1d), others identified "locked zones" like Zabargad Island (Courtillot, 1982).

The Red Sea was later divided into southern, central, and northern provinces (Cochran, 1983). Bonatti et al. (1984) found MORB basalt at Nereus Deep (Fig.1d) indicating spreading at 2-3 Ma. Girdler (1985) proposed a three-phase evolution linked to the Aqaba-Dead Sea shear. Investigations at 22°N to 25°N identified quasi-oceanic crust (LaBrecque and Zitellini, 1985), while Bicknell et al. (1986) and Bonatti (1987) debated the semantics of the controversy. Research continued to show varied initiation times, from 10–12 Ma (Izzeldin, 1987) to a 200 km fracture rift phase (Joffe and Garfunkel, 1987).

1.1.5. Tectonic Inheritance and Integrated Structural Models

Recent ESP data show oceanic-type velocities at 26°N despite thinned continental characteristics (Gaulier et al., 1988; Martinez and Cochran, 1988). Detailed mapping of Inter-Trough Zones (ITZ) and transverse structures (Izzeldin, 1989; Guennoc et al., 1990) attempted to resolve the validity of the three proposed models (Uchupi and Ross, 1990; Girdler, 1991). Gravity studies emphasized crustal thickening (Makris and Rihm, 1991), while the Najd Shear System and Onib-Hamisana/Baraka sutures (Fig.1e) were identified as pre-existing infrastructure controlling the rift (Makris and Henke, 1992).

Bosworth et al. (1996) noted the only known off-shore pre-rift Zabargad Formation, while the northern province was found to be amagmatic during rifting (Bosworth and McClay, 2001; Cochran, 2005). Early magmatism (29.9-28.7 Ma) was linked to the Afar plume (Bosworth, 2015; Bosworth and Stockli, 2016), with lithospheric thinning following at 15-12 Ma (Blanchette et al., 2018). Recent data suggest rifting initiated in the south (Bosworth et al., 2020), involving transtensional structures (Issachar et al., 2022) and oblique Mid-Ocean Ridges (Delaunay et al., 2023).

2. Methodology

To resolve inconsistencies in previous models, this study employs a Multi-Proxy Geospatial Integration workflow. We synthesized five datasets in one georeferenced database for integration and interpretation to identify crustal boundaries:

1. **Potential Field Analysis (Figs. 1a-b):** Gravity and magnetic anomaly maps were utilized to delineate the Median Ridge Valley (MRV) and identify lateral offsets in magnetic (Fig.4a) and magnetic faults lineations (Fig.3 a-f). Also, Identifying the magnetic stripes.

- **Criteria for Magnetic Stripe Identification**: Central to this analysis is the identification of magnetic stripes (Fig. 3f). Following the hypothesis introduced by Vine and Matthews (1963), we define these *stripes* based on the criteria of *linearity, bilateral symmetry, and organized polarity*. On georeferenced magnetic intensity maps, these appear *as elongated, strike-parallel "ribbons"* of *alternating positive and negative anomalies*. This pattern is fundamentally distinct from magmatic intrusions, which typically manifest as *discrete, high-amplitude "blobs" or irregular circular clusters with localized signatures*. While an intrusion represents a singular, stagnant magmatic event, magnetic stripes serve as a *"geomagnetic tape recorder," capturing the Earth's polarity reversals during continuous crustal accretion at a spreading center.*

2. **Qualitative Interpretation (Fig.3 a-f):** The gravity and magnetic data are interpreted qualitatively by focusing on lateral changes in anomaly patterns and its correspondence with georeferenced tectonic domains and sutures (Fig.4a). The data are interpreted in a comparative framework rather than through forward or inverse modeling, emphasizing spatial coherence and anomaly continuity across the Red Sea rift.

3. **Seismic Velocity Correlation (Fig. 2):** We reconstructed a 1900 km compiled seismic refraction profile based on VEMA-Atlantis data (Fig.1c and Fig.2). Crustal types were categorized by velocities : oceanic/intrusive crust (V> 6.4 km/s) and continental crust (V < 6.4 km/s). Accordingly, these seismic datasets serve as independent constraints on interpretations derived from gravity and magnetic observations and are used to evaluate whether

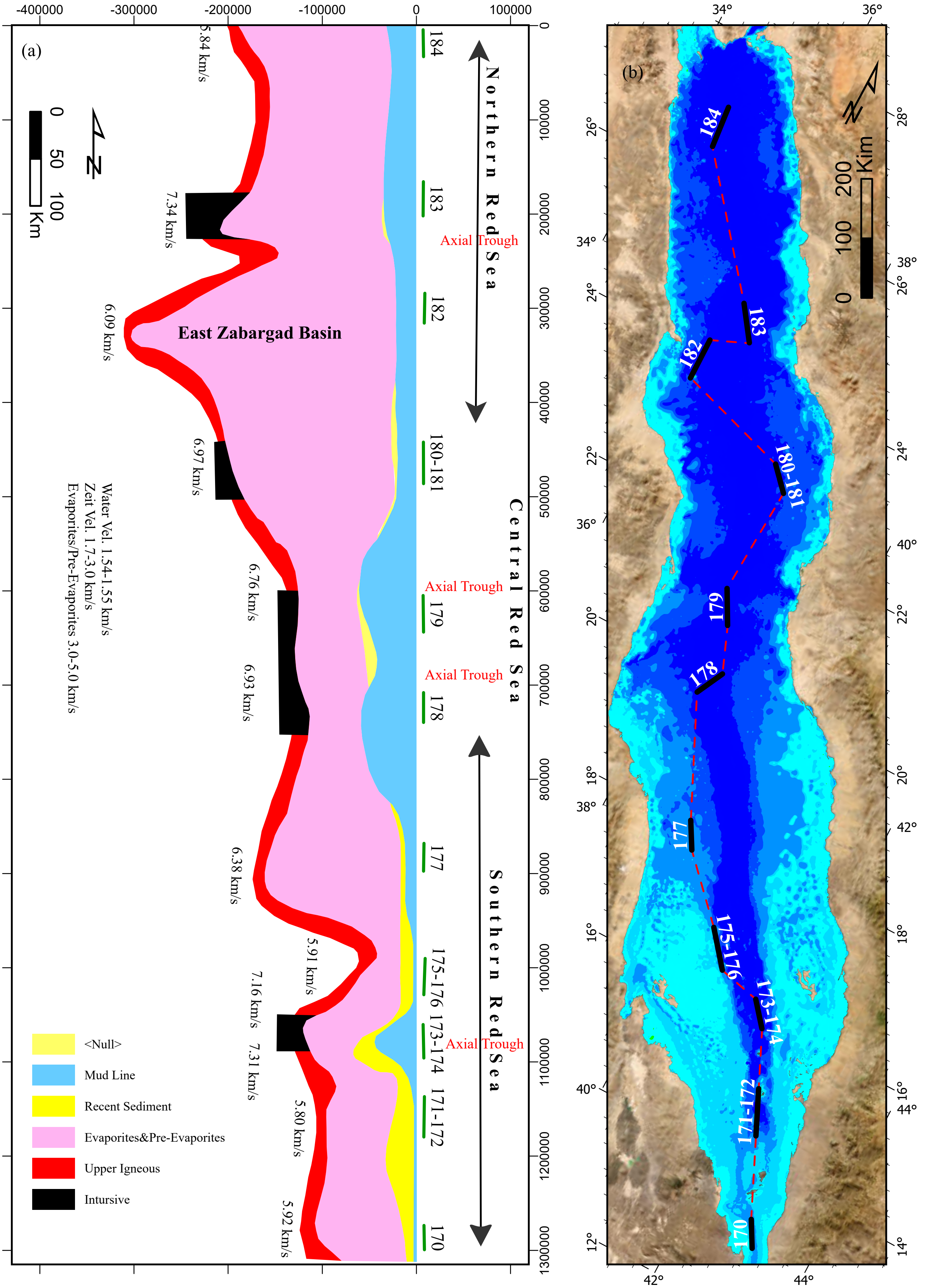

Figure 2: Regional 1900 km Seismic Refraction. (a) A synthesized and reconstructed crustal cross-section spanning 1900 km along the Red Sea axis, integrated from legacy seismic refraction data (Drake and Girdler, 1964; Tramontini and Davies, 1969; Cochran, 1983).
(b) Spatial distribution of the 1958 VEMA-Atlantis seismic refraction stations (indicated in black). The model distinguishes between two primary crustal velocity domains: Continental Basement, characterized by velocities of 5.5–6.4 km/s, and Oceanic/Intrusive Architecture, defined by higher velocities of 6.7–7.31 km/s. These velocity provide key support for identifying the boundaries of the three structural provinces proposed in this study.

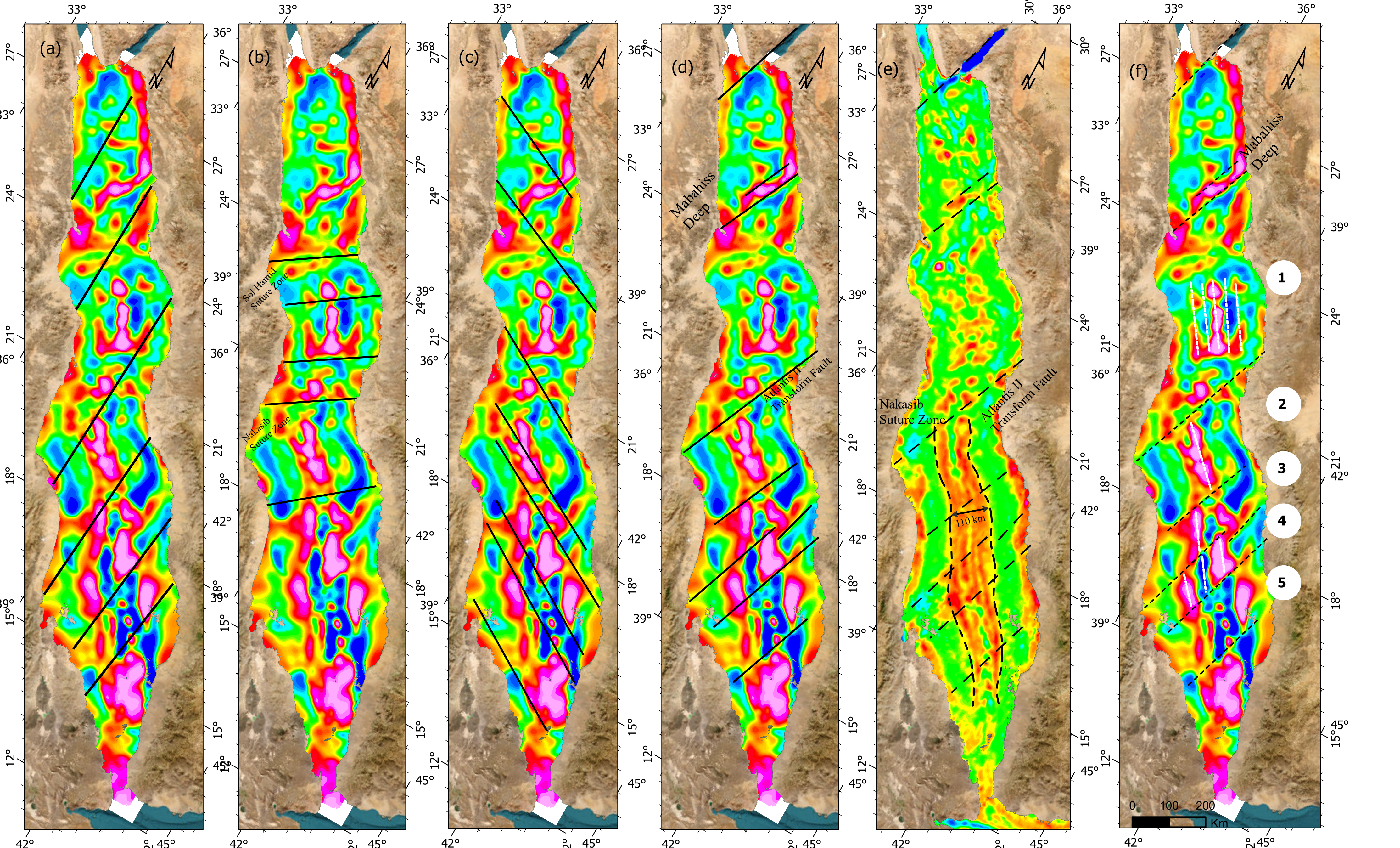

Figure 3: Integrated Tectonic and Magnetic Fabric of the Red Sea. Maps (a-d) delineate the four primary structural trends:(a) N-S basement faults; (b) Inherited Precambrian Suture trends; (c) Najd Shear System trends; and (d) the Aqaba-Dead Sea transform-related faults. Map (e) illustrates the Southern Red Sea axial ridge, characterized by a high-amplitude gravity anomaly (110 km width; 850 km strike length), which terminates abruptly at the Nakasib Suture Zone, marking a major crustal boundary. Map (f) highlights five distinct groups of linear magnetic stripes identified along the central and southern provinces. These white dashed elongated signatures are interpreted as Vine-Matthews stripes, representing organized seafloor spreading. Notably, these magnetic stripes are intersected and segmented by the interpreted strike-slip faults (derived from trends in maps d), demonstrating that inherited Precambrian infrastructure and transform tectonics directly control the lateral offset and fragmentation of the oceanic crust.

observed geophysical anomalies are consistent with continental, transitional, or oceanic crustal characteristics velocity.

4. **Bathymetric Analysis (Figs. 1c-d):** Bathymetry was analyzed to identify the physical morphology of the axial trough and deeps. Also, the bathymetric data were used to characterize basin segmentation, depth variations along the rift axis. The bathymetry serves as the surface expression and were incorporated into the geospatial database and analyzed together with geophysical anomalies to assess correspondence between morphological and subsurface features. We used these seafloor signatures to distinguish the organized spreading centers.

5. **Tectonic Inheritance Mapping (Fig. 1e):** Onshore Precambrian suture zones (e.g., Nakasib and Sol Hamid) were projected offshore (Fig.4a and b) to evaluate their role as boundaries for modern rift segmentation and its relation to offshore magnetic and gravity anomalies. The synthesized georeferenced geological map (Fig.1e) delineates suture zones, inherited continental terranes and exposed crustal domains.

6. **Modeling Correlation (Fig.4e):** We applied the 1 cm/yr spreading rate established by Vine (1966) to a newly identified 250 km magnetic profile (A-A') (Fig.4b) in the central Red Sea.

7. **Stratigraphic Integration:** The Miocene "S-reflector" (5 Ma) and the Jeddah-1 well (location, Fig.1c) data were used as chronological anchors to calibrate the possible ages of the identified elongated, successive magnetic stripes in central Red Sea (Fig.3f and Fig.4b).

A cornerstone of this multi-proxy methodology was the strict geospatial of all heterogeneous datasets within a high-resolution and fully georeferenced framework. By integrating geophysical data, bathymetric, and stratigraphic maps into a single spatial coordinate system, the analysis moved beyond conventional one-dimensional interpretations toward a genuinely multidimensional integration. This spatial coherence was critical for validating the landward continuation of Proterozoic suture zones against offshore magnetic lineations. In doing so, it converted previously isolated observations into a unified, spatially consistent tectonic framework, enabling precise delineation of crustal boundaries and robust correlation of displacements across the various Red Sea provinces.

Newly interpreted four dominant structural trends (Fig.3 a-d) that govern the Red Sea's segmentation: The North-South fault trend (a), the Precambrian Suture trend (b), the Najd Shear System trend (c), and the Aqaba transform trend (d). The interpretation reveals that these inherited basement grains, particularly the Nakasib and Sol Hamid sutures (Fig.1e, Fig.3b and Fig.4a), act as fundamental boundaries that terminate or offset magnetic lineations, proving that the rift's propagation is controlled by ancient lithospheric architecture.

Figure 4 synthesize these datasets and illustrate how spatial correlations inform an alternative crustal evolution model for the Red Sea rift. The interpretations emphasize inherited lithospheric structure and suture control on rift development, rather than assuming uniform oceanic spreading along the rift axis. Interpretation strategy is based on the coherence or mismatch between the datasets.

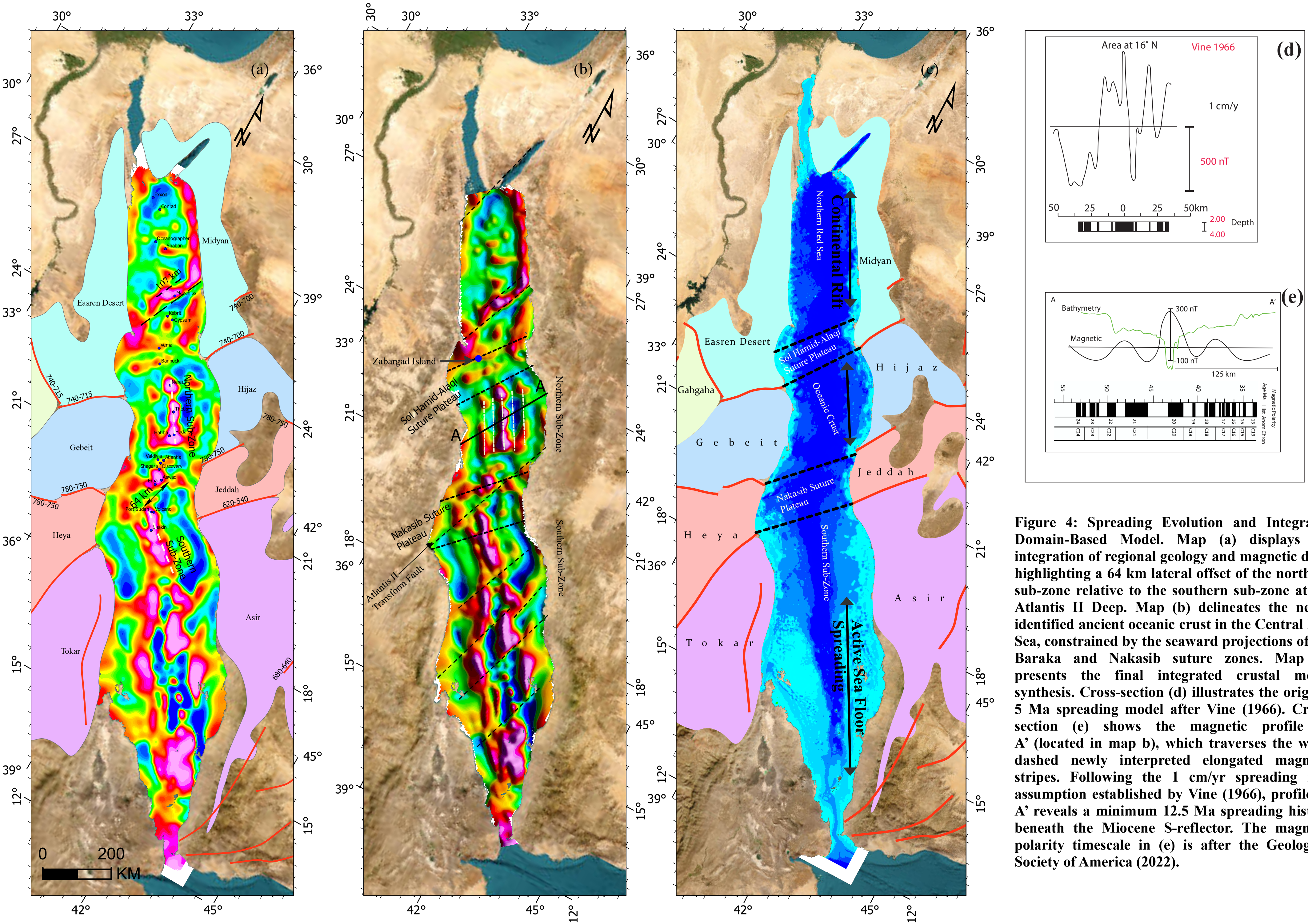

Figure 4: Spreading Evolution and Integrated Domain-Based Model. Map (a) displays the integration of regional geology and magnetic data, highlighting a 64 km lateral offset of the northern sub-zone relative to the southern sub-zone at the Atlantis II Deep. Map (b) delineates the newly identified ancient oceanic crust in the Central Red Sea, constrained by the seaward projections of the Baraka and Nakasib suture zones. Map (c) presents the final integrated crustal model synthesis. Cross-section (d) illustrates the original 5 Ma spreading model after Vine (1966). Cross-section (e) shows the magnetic profile A-A' (located in map b), which traverses the white dashed newly interpreted elongated magnetic stripes. Following the 1 cm/yr spreading rate assumption established by Vine (1966), profile A-A' reveals a minimum 12.5 Ma spreading history beneath the Miocene S-reflector. The magnetic polarity timescale in (e) is after the Geological Society of America (2022).

3. Results

3.1. Geophysical Characterization of Structural Provinces

The integration of georeferenced gravity, magnetic, and seismic datasets delineates three distinct structural provinces and four dominant structural trends (N-S, Precambrian Suture, Najd Shear, and Aqaba transform) within the Red Sea basin:

- **Southern Province (13°30'N to 18°30'N):** Defined by elongated, continuous magnetic and gravity lineations extending over 800 km (Fig. 3e-f and Fig. 4a-b). These lineations show high spatial correlation with a high-amplitude positive gravity anomaly (110 km width, Fig.3e) situated directly over the Median Ridge Valley (MRV). Seismic refraction data (Lines 170-178) recorded high velocities > 6.4 km/s, identifying a robust oceanic crustal architecture.
- **Central Province (18°30'N to 23°N):** Exhibits magnetic organized polarity signatures (Fig.3f); however, a divergence is observed north of the Heya terrane (Fig.4a and b), where corresponding gravity anomalies are absent (Fig.3e). While high seismic velocities (6.76 to 6.97 km/s) persist along the MRV (Lines 179-181), and bathymetric data indicates increasingly irregular morphological signatures.
- **Northern Province (23°N to 27°30'N):** (Fig.4a and b) Unlike the southern provinces, the Northern Red Sea maintains the distinct characteristics of an amagmatic continental rift. The presence of pre-rift sequences, such as the Zabargad Formation, and seismic refraction velocities consistently below 6.4 km/s, lend a hand in identifying this domain as continental basement. We interpret the discrete, low-amplitude magnetic patterns observed here as evidence of diffuse extension rather than organized seafloor spreading.

3.2. Identification of Vine-Matthews Stripes and Structural Offsets

Geospatial analysis identifies five distinct clusters of linear magnetic anomalies along the Central and Southern provinces (Fig. 3f). These white dashed elongated signatures features are interpreted as Vine-Matthews stripes, characterized by strike-parallel continuity with approximate lengths of 220 km, 220 km, 150 km, and 100 km for Groups 1 through 4, respectively. In contrast, Group 5 exhibits a highly fragmented architecture, where the magnetic stripes are intersected and segmented by small scale strike-slip faults. This segmentation lends a hand in demonstrating how inherited Precambrian infrastructure directly controls the lateral displacement and modern geometry of the oceanic crust. These Vine-Matthews stripes-like, representing organized seafloor spreading rather than discrete continental intrusions.

A prominent structural discontinuity occurs at the Atlantis II Deep (20°30'N), terminates abruptly the gravity at the Nakasib Suture Zone (Fig.3e), marking a major crustal boundary. The magnetic anomaly axis is laterally offset by a distance of 64 km (Fig.4a) between the northern and southern sub-zones (white dashed lines Fig.4a). Geospatial integration confirms that this offshore offset aligns with the seaward projection of the onshore Baraka left-lateral suture (Fig. 4a and b).

3.3. Stratigraphic Analysis and Magnetic Correlation

Analysis of magnetic profile A-A' reveals a sequence of organized polarity reversals (250 km wide and 220 km strike length) (Fig.4b and e) situated beneath the Miocene S-reflector. Based on the 1 cm/yr spreading rate established by Vine (1966), the identified magnetic stripes represent a spreading duration of 12.5 Ma. Calibration against the 5 Ma of the S-reflector yields a total minimum age of 17.5 Ma for this segment. Magnetic correlation with the geomagnetic polarity timescale (GSA, 2022, Fig.4e) shows a high degree of correlation for a 12 Ma interval, spanning chrons C20 through C24. Furthermore, stratigraphic data from the Jeddah-1 well identifies 100 m of volcanic sequences within the Eocene interval.

4. Discussion

4.1. Southern Red Sea Province: Limits of Oceanic Propagation

The Southern Red Sea axial ridge is characterized by straight-sided bathymetric troughs (fig.1d). While prevailing models suggest this crust formed over the last 3-5 Ma , our integrated analysis challenges the 40 Ma oceanic crust hypothesis. A landward continuation of that 40 Ma model creates a stratigraphic paradox, as it would require Jurassic formations to overlie Eocene oceanic crust, a geological impossibility.

Furthermore, the "shore-to-shore" oceanic hypothesis is contradicted by our synthesized potential field data. Gravity-dense rock signatures are strictly confined to the Median Ridge Valley (MRV, Fig.3e). This zone of active oceanization terminates abruptly at 20°30'N (Fig.3e), precisely where it meets the Nakasib Suture Zone. We interpret this as evidence that oceanic crust south of 20°30'N is restricted to the axial trough , with its early propagation heavily dictated by the impingement of the Afar plume at ~34 Ma.

4.2. Central Red Sea: Suture-Controlled Offsets and the 17.5 Ma Oceanic Crust

The Central Province provides the most compelling evidence for a Domain-Based Model. While previous studies characterized deeps like Nereus as young "oceanization cells" (2-3 Ma) , our discovery of organized Vine-Matthews stripes (Fig.3f and Fig.4b) beneath the undisturbed Miocene "S-reflector" mandates a much older origin. Instead, the area between the Sol Hamid and Nakasib sutures represents a stage where isolated oceanic deeps of active seafloor spreading are embedded within an ancient oceanic crustal. Because the 5 Ma reflector remains structurally intact across these anomalies, the underlying oceanic crust must pre-date the Pliocene. By applying the 1 cm/yr spreading rate to the georeferenced Profile A-A' (Fig.4b and e), we estimate a minimum age of 17.5 Ma. The volcanic sequences identified in the Jeddah-1 wells likely represent localized igneous intrusions at the transition to the Central Province.

This province is not uniform; it is segmented by a 64 km lateral offset at the Atlantis II Deep (Fig.4a). We interpret this offset as an expression of tectonic inheritance. The alignment between this 64 km magnetic shift and the seaward continuation of the Baraka Suture-where the shoreline shifts northward suggests that Precambrian infrastructure forced the rift to offset laterally during its evolution.

4.3. Northern Red Sea: Amagmatic Rifting and Inherited Architecture

Unlike the magmatic southern provinces, the Northern Red Sea maintains characteristics of an amagmatic continental rift. The presence of pre-rift sequences (Zabargad Formation) and seismic velocities below 6.4 km/s provides a helping hand in identifying this as continental basement. We interpret the discrete, low-amplitude magnetic patterns as evidence of diffuse extension rather than seafloor spreading. Regarding the interpreted oceanic boundaries proposed by Gaulier et al. (1988) via fifteen Expanding Spread Profiles (ESPs), we highlight a significant ambiguity in seismic interpretation. Specifically, the high-velocity and high-density signatures identified in the North are not exclusive to oceanic crust. We posit that if the diverse Neoproterozoic basement of the Egyptian Eastern Desert-including its ophiolites, ophiolitic mélange, granitoids, metavolcanics, and gneiss complexes-were submerged and subjected to identical seismic acquisition, the resulting velocity profiles would be indistinguishable from those reported by Gaulier. Consequently, seismic velocity alone provides a helping hand but is not a definitive diagnostic for oceanic crust in the absence of organized magnetic stripes.

4.4. Discussion Synthesis: Inherited Evolution

The integration of geological and geophysical correlations indicates that Red Sea crustal evolution is highly segmented and structurally inherited rather than a uniform process. Our model (Fig.4c) reveals three distinct evolutionary behaviors:

- **Southern:** Axial-only spreading constrained by the Nakasib Suture.
- **Central:** Ancient (minimum 17.5 Ma) oceanic domains constrained by the Sol Hamid Suture.
- **Northern:** Continental rifting governed by Neoproterozoic structural grain and the Aqaba-Dead Sea transform system.

Fundamentally, these findings prove that the Red Sea is a segmented rift , where the timing and geometry of crustal growth are dictated by the inherited architecture of the Arabian-Nubian Shield.

5. Conclusion

The present work provides a new combined model (Fig.4c) for the opening of the Red Sea by integrating surface geology, magnetic, gravity, bathymetric, and seismic refraction data. Our findings indicate that the Red Sea did not develop through a single, continuous event, but rather through separate domains and distinct phases governed by inherited Precambrian architecture (Fig.4a, b and c).

- **Ancient Oceanic Crust Discovery**: This study identifies a newly interpreted oceanic crustal segment within the central Red Sea province, where seafloor spreading occurred over a span of 12.5 Ma. When calibrated with the top Miocene S-reflector and Jeddah-1 well data, the total minimum age of 17.5 Ma strongly correlates with magnetic anomaly chrons and polarities of Eocene age. This suggests a significantly older initiation of oceanic crustal formation in the central Red Sea than previously modeled.
- **Suture-Controlled Segmentation**: The structural architecture of the basin is defined by the offshore extension of two inherited Proterozoic suture zones that divide the Red Sea into three distinct provinces. These infrastructures controlled the propagation and segmentation of the rift throughout its evolution:
- **The Nakasib Suture**: Separates the currently active seafloor spreading in the southern province from the oceanic crust of the central Red Sea.
- **The Sol Hamid-Alaqi Suture**: Marks the boundary between the central oceanic province and the northern Red Sea.
- **Distinct Crustal Identities**: The northern province is characterized by discrete, scattered magnetic anomalies and a notable absence of magnetic and gravity lineation patterns, signifying a diffuse continental rift. This stands in sharp contrast to the organized seafloor spreading signatures identified in the central and southern provinces.

Conclusively, this domain-based evolution explains the long-standing inconsistencies in Red Sea. By recognizing the role of inherited tectonic grains, this study provides a framework for understanding how ancient continental structures dictate the geometry and timing of modern oceanic drift. Future research should focus on high-resolution sampling of these older magnetic stripes to further refine the timing of the Red Sea's initial pulse of seafloor spreading.

Data availability

The regional geophysical datasets supporting the findings of this study are publicly available. Potential field and bathymetric data were integrated from the NOAA National Centers for Environmental Information (https://www.ngdc.noaa.gov), the UCSD Topographic/Bathymetric database (https://topex.ucsd.edu), and the World Digital Magnetic Anomaly Map (WDMAM v2.1) repository (http://www.wdmam.org). Specific processed datasets or geospatial integrations generated during the current study are available from the corresponding author upon reasonable request.

Author contributions

KF: Conceptualization, Methodology, Data Acquisition, Formal Analysis, and Writing-Original Draft. AE: Data Curation, Writing-Review & Editing, and Technical Supervision.

Competing interests

The authors declare no competing interests.

Acknowledgement

We thank Mr. Dia Mahmoud, GEOPEX Ltd. and Dr. Hussein Hammouda, Ex-Chairman of Egyptian Mineral Resources Authority, for their help in digitizing the old Red Sea magnetic and gravity paper sheets. Special thanks to the late Dr. Wafik Mishrif for his support and encouragement in collecting most of fabulous magnetic and gravity sheets over Gulf of Suez and Red Sea. Thanks to The National Geophysical Data Center (NGDC) for delivering the copy of gravity and magnetic data acquired over Red Sea. Thanks to Dr. Hans A. Roeser for providing his own gravity and magnetic material of 1975, 1976 and 1980.

Author information

Name: Farhoud, Khamis

Position: Study and Seismic Team Lead, Anton Oil, Majnoon Oil Field, Basra, Iraq

Email: kh_farhoud@hotmail.com

Phone No.: +201116055558

Name: El-Barkooky, Ahmed N.

Position: Professor in the Geology Department of Cairo University

Email: abarkook@cu.edu.eg

References

Abdel-Gawad, M.: Geological structures of the Red Sea area inferred from satellite pictures, in: Hot Brines and Recent Heavy Metal Deposits in the Red Sea, Springer, 25–37, https://doi.org/10.1007/978-3-662-28603-6_5, 1969.

Ahmed, S. S.: Geology and petroleum prospects in the eastern Red Sea, AAPG Bull., 56, 707–719, https://doi.org/10.1306/819A407A-16C5-11D7-8645000102C1865D, 1972.

Allan, T. D.: Magnetic and gravity fields over the Red Sea, Philos. Trans. R. Soc. Lond. A, 261, 153–180, https://doi.org/10.1098/rsta.1970.0030, 1970.

Allan, T. D.: A Bathymetric Chart of the Red Sea. International Hydrographic Review, 43, 33–36, 1966.

Bicknell, J. D., Macdonald, K. C., Miller, S. P., Lonsdale, P. F., and Becker, K.: Tectonics of the Nereus Deep, Red Sea: A deep-tow investigation of a site of initial rifting, J. Geophys. Res., 91, 131–148, https://doi.org/10.1007/bf00338225, 1986.

Blanchette, A. R., Klemperer, S. L., Mooney, W. D., and Zahran, H. M.: Two-stage Red Sea rifting inferred from mantle earthquakes in Neoproterozoic lithosphere, Earth Planet. Sci. Lett., 497, 92–101, https://doi.org/10.1016/j.epsl.2018.05.048, 2018.

Bonatti, E.: Punctiform initiation of seafloor spreading in the Red Sea during transition from a continental to an oceanic rift, Nature, 316, 33–37, https://doi.org/10.1038/316033a0, 1985.

Bonatti, E.: Rifting or drifting in the Red Sea?, Nature, 330, 962–963, https://doi.org/10.1038/330692a0, 1987.

Bonatti, E., Colantoni, P., Della Vedova, B., and Taviani, M.: Geology of the Red Sea transitional region (22° N–25° N), Oceanol. Acta, 7, 385–398, 1984.

Bosworth, W. and Stockli, D. F.: Early magmatism in the greater Red Sea, Can. J. Earth Sci., 53, 1158–1176, https://doi.org/10.1139/cjes-2016-0019 , 2016.

Bosworth, W. and McClay, K. R.: Structural and stratigraphic evolution of the Gulf of Suez Rift, Egypt, in: Peri-Tethys Memoir 6, Springer, 567–606, 2001.

Bosworth, W., Darwish, M., Crevello, P., Taviani, M., and Marshak, S.: Stratigraphic and structural evolution of Zabargad Island (Red Sea, Egypt) since the Early Cretaceous, Proc. 3rd Int. Conf. Geol. Arab World, Cairo Univ., 161–190, 1996.

Bosworth, W., Khalil, S. M., Ligi, M., Stockli, D. F., and McClay, K. R.: The northern Red Sea, in: Geology of Egypt, Springer, 344–369, https://doi.org/10.1007/978-3-030-15265-9_9 , 2020.

Bosworth, W.: Geological evolution of the Red Sea: Historical background, review, and synthesis, Springer Earth Syst. Sci., 45–78, https://doi.org/10.1007/978-3-662-45201-1_3 , 2015.

Brown, C. and Girdler, R. W.: Structure of the Red Sea at 20° N from gravity data and its implications for continental margins, Nature, 298, 51–53, https://doi.org/10.1038/298051a0 ,1982.

Bunter, M. A. G., Debretsion, T., and Woldegiorgis, L.: New developments in the pre-rift prospectivity of the Eritrean Red Sea, J. Petrol. Geol., 21, 73–100, https://doi.org/10.1111/j.1747-5457.1998.tb00792.x, 1998.

Carey, S. W.: A tectonic approach to continental drift, in: Continental Drift: A Symposium, University of Tasmania, Hobart, 177–355, 1958.

Cochran, J. R.: A model for development of Red Sea, AAPG Bull., 67, 41–69, https://doi.org/10.1306/03B5ACBE-16D1-11D7-8645000102C1865D, 1983.

Cochran, J. R.: Northern Red Sea: Nucleation of an oceanic spreading center within a continental rift, Geochem. Geophys. Geosyst., 6, Q03006, https://doi.org/10.1029/2004gc000826, 2005.

Courtillot, V.: Propagating rifts and continental breakup, Tectonics, 1, 239–250, https://doi.org/10.1029/TC001i003p00239 ,1982.

Crane, K. and Bonatti, E.: The role of fracture zones during early Red Sea rifting: Structural analysis using space shuttle radar and LANDSAT imagery, J. Geol. Soc. Lond., 144, 407–420, https://doi.org/10.1144/gsjgs.144.3.0407, 1987.

Delaunay, A., Baby, G., Fedorik, J., Afifi, A. M., Tapponnier, P., and Dyment, J.: Structure and morphology of the Red Sea, from the mid-ocean ridge to the ocean-continent boundary, Tectonophysics, 849, https://doi.org/10.1016/j.tecto.2023.229728 , 2023.

Dixon, C. L., Stern, R. J., and Hussein, I. M.: Control of Red Sea rift geometry by Precambrian structures, Tectonics, 6, 551–571, https://doi.org/10.1029/TC006i005p00551, 1987.

Drake, C. L. and Girdler, R. W.: A geophysical study of the Red Sea, Geophys. J., 8, 473–495, https://doi.org/10.1111/j.1365-246X.1964.tb06303.x, 1964.

Drake, C. L., Girdler, R. W., and Landisman, M.: Geophysical measurements in the Red Sea, Proc. Int. Oceanogr. Congr., 20, 1959.

Farquharson, W. I.: Topography, with an appendix on magnetic observations, Scientific Reports of the John Murray Expedition 1933-34, 1, 43–61, 1935.

Gaulier, J. M., Le Pichon, X., Lyberis, N., Avedik, F., Geli, L., Moretti, I., Deschamps, A., and Hafez, S.: Seismic study of the crust of the northern Red Sea and Gulf of Suez, Tectonophysics, 153, 55–88, https://doi.org/10.1016/0040-1951(88)90007-8 , 1988.

Gettings, M. E.: Delineation of the continental margin of the southern Red Sea from new gravity evidence, Saudi Arab. Dir. Gen. Miner. Res. Bull., 2, K1–K11, 1977.

Girdler, R. W. and Evans, T. R.: Red Sea heat flow, Geophys. J. R. Astron. Soc., 51, 245–251, https://doi.org/10.1111/j.1365-246x.1977.tb04199.x , 1977.

Girdler, R. W.: A review of Red Sea heat flow, Philos. Trans. R. Soc. Lond. A, 267, 359–368, https://doi.org/10.1098/rsta.1970.0032, 1970.

Girdler, R. W.: Earth satellites, terrestrial heat flow, mantle convection and the location of extensional and compressional features on the Earth's surface, Proc. Geol. Assoc., 78, 165–178, https://doi.org/10.1016/s0016-7878(67)80042-7 , 1967.

Girdler, R. W.: Problems concerning the evolution of oceanic lithosphere in the northern Red Sea, Tectonophysics, 116, 109–122, https://doi.org/10.1016/0040-1951(85)90224-0, 1985.

Girdler, R. W.: The case for oceanic crust beneath the Red Sea, Tectonophysics, 198, 275–278, https://doi.org/10.1016/0040-1951(91)90155-L, 1991.

Girdler, R. W.: The relationship of the Red Sea to the East African Rift System, Q. J. Geol. Soc. Lond., 114, 79–105, https://doi.org/10.1144/gsjgs.114.1.0079, 1958.

Girdler, R. W. and Peter, G.: An example of the importance of natural remanent magnetization in the interpretation of magnetic anomalies, Geophys. Prospect., 8, 474–483, https://doi.org/10.1111/j.1365-2478.1960.tb01730.x, 1960.

Girdler, R. W. and Harrison, J. C.: Submarine gravity measurements in the Atlantic, Indian Ocean, Red Sea and Mediterranean Sea, Proc. R. Soc. Lond. A, 239, 202, https://doi.org/10.1098/rspa.1957.0033, 1957.

Girdler, R. W. and Styles, P.: Two-stage Red Sea floor spreading, Nature, 330, 716–721, https://doi.org/10.1038/247007a0, 1974.

Girdler, R. W., Brown, C., Noy, D. J. M., and Styles, P.: Geophysical survey of the westernmost Gulf of Aden, Philos. Trans. R. Soc. Lond. A, 298, 1–43, https://doi.org/10.1098/rsta.1980.0239, 1980.

Girdler, R. W. and Southren, T. : Structure and evolution of the northern Red Sea, Nature, 330, 716–721, https://doi.org/10.1038/330716a0, 1987.

Guennoc, P., Pautot, G., Le Quentrec, M.-F., and Coutelle, A.: Structure of an early oceanic rift in the northern Red Sea, Oceanol. Acta, 13, 145–155, 1990.

Hofmann, C. et al.: Timing of the Ethiopian flood basalt event and implications for plume birth and global change, Nature, 389, 838–841, https://doi.org/10.1038/39853, 1997.

Hughes, G. W. and Johnson, R. S.: Lithostratigraphy of the Red Sea region, GeoArabia, 10, 49–126, https://doi.org/10.2113/geoarabia100349, 2005.

Issachar, R., Ebbing, J., and Dilixiati, Y.: New magnetic anomaly map for the Red Sea reveals transtensional structures associated with rotational rifting, Sci. Rep., 12, 5757, https://doi.org/10.1038/s41598-022-09770-0, 2022.

Izzeldin, A. Y.: Seismic, gravity and magnetic surveys in the central part of the Red Sea, Tectonophysics, 143, 269–306, https://doi.org/10.1016/0040-1951(87)90214-9, 1987.

Izzeldin, A. Y.: Transverse structures in the central Red Sea and implications for early oceanic accretion, Geophys. J., 96, 117–129, https://doi.org/10.1111/j.1365-246X.1989.tb05254.x, 1989.

Jarrige, J. J. et al.: Inherited discontinuities and Neogene structure of the Gulf of Suez and NW Red Sea, Philos. Trans. R. Soc. Lond. A, 317, 129–139, https://doi.org/10.1098/rsta.1986.0029, 1986.

Joffe, S. and Garfunkel, Z.: Plate kinematics of the circum–Red Sea: A re-evaluation, Tectonophysics, 141, 5–23, https://doi.org/10.1016/0040-1951(87)90171-5, 1987.

Knott, S. T., Bunce, E. T., and Chase, R. L.: Red Sea seismic reflection studies, Geol. Surv. Can. Pap., 66-14, 33–61, https://doi.org/10.4095/103358, 1966.

LaBrecque, J., Kent, D. V., and Cande, S. C.: Revised magnetic polarity time scale for Late Cretaceous and Cenozoic time, Geology, 5, 330–335, https://doi.org/10.1130/0091-7613(1977)5<330:rmptsf>2.0.co;2, 1977.

LaBrecque, J. L. and Zitellini, N.: Continuous seafloor spreading in the Red Sea, AAPG Bull., 69, 513–524, https://doi.org/10.1306/AD46251F-16F7-11D7-8645000102C1865D, 1985.

Le Pichon, X. and Francheteau, J.: Plate tectonic analysis of the Red Sea–Gulf of Aden area, Tectonophysics, 46, 369–406, https://doi.org/10.1016/0040-1951(78)90214-7, 1978.

Lowell, J. D. and Genik, G. J.: Sea-floor spreading and structural evolution of the southern Red Sea, AAPG Bull., 56, 247–259, https://doi.org/10.1306/819a3e56-16c5-11d7-8645000102c1865d, 1972.

Makris, J. and Henke, C. H.: Pull-apart evolution of the Red Sea, J. Petrol. Geol., 15, 127–134, https://doi.org/10.1111/j.1747-5457.1992.tb00958.x, 1992.

Makris, J. and Rihm, R.: Shear-controlled evolution of the Red Sea, Tectonophysics, 198, 441–466, https://doi.org/10.1016/0040-1951(91)90166-p, 1991.

Martinez, F. and Cochran, J. R.: Structure and tectonics of the northern Red Sea, Tectonophysics, 150, 1–32, https://doi.org/10.1016/0040-1951(88)90293-4, 1988.

McKenzie, D. P., Davies, D., and Molnar, P.: Plate tectonics of the Red Sea and East Africa, Nature, 226, 243–248, https://doi.org/10.1038/226243a0, 1970.

Nashaat, M. and Mokhtar, A.: Salt dynamics impact on hydrocarbon generation in the Red Sea, EGPC Explor. Semin., 340–351, 1996.

Owen, L.: Origin of the Red Sea depression, AAPG Bull., 22, 1217–1223, https://doi.org/10.1306/3d932fe0-16b1-11d7-8645000102c1865d, 1938.

Phillips, J. and Ross, D. A.: Continuous seismic reflection profiles in the Red Sea, Philos. Trans. R. Soc. Lond. A, 267, 143–152, https://doi.org/10.1098/RSTA.1970.0029, 1970.

Phillips, J. D., Woodside, J., and Bowin, C. O.: Magnetic and gravity anomalies in the central Red Sea, in: Hot Brines and Recent Heavy Metal Deposits in the Red Sea, Springer, 98–113, https://doi.org/10.1007/978-3-662-28603-6_10, 1969.

Quennell, A. M.: Tectonics of the Dead Sea rift, Int. Geol. Congr., 20, 385–405, 1956.

Quennell, A. M.: Tectonics of the Dead Sea rift, Assoc. Afr. Geol. Surv., 385–408, 1959.

Roeser, H. A.: Detailed magnetic survey of the southern Red Sea, Geol. Jahrb., 13, 131–153, 1975.

Roger, C., Searle, R., and Ross, D. A.: Geophysical study of the Red Sea axial trough, Geophys. J. R. Astron. Soc., 43, 555–572, https://doi.org/10.1111/j.1365-246x.1975.tb00647.x, 1975.

Sestini, J.: Cenozoic stratigraphy and depositional history of the Red Sea coast, Sudan, AAPG Bull., 49, 1452–1472, https://doi.org/10.1306/A6633726-16C0-11D7-8645000102C1865D, 1965.

Stieltjes, L.: Evolution tectonique recente du rift d'Asal, Rev. Geogr. Phys. Geol. Dyn., 15, 425–436, 1973.

Stoffers, P. and Ross, D. A.: Sedimentary history of the Red Sea, Woods Hole Oceanogr. Inst. Contrib., 3168, 849–865, https://doi.org/10.2973/dsdp.proc.23.123.1974, 1974.

Tazieff, H.: Une recente campagne oceanographique dans la mer Rouge, Bull. Soc. Belge Geol., 61, 84–90, 1952.

Tramontini, C. and Davies, D.: Seismic refraction survey in the Red Sea, Geophys. J., 17, 225–241, https://doi.org/10.1111/j.1365-246x.1969.tb02323.x, 1969.

Uchupi, E. and Ross, D. A.: The geologic enigma of the Red Sea rift, in: Facets of Modern Biogeochemistry, Springer, 52–61, 1990.

Vening Meinesz, F. A.: Gravity expeditions at sea, 1923–1932, Vol. II, Netherlands Geodetic Commission, Delft, https://doi.org/10.54419/3us2nj, 1934.

Vine, F. J.: Spreading of the ocean floor: New evidence, Science, 154, 1405–1415, https://doi.org/10.1126/science.154.3755.1405, 1966.

Vine, F. J. and Matthews, D. H.: Magnetic anomalies over ocean ridges, Nature, 199, 947–949, https://doi.org/10.1038/199947a0, 1963.

Von Triulzi, A. E.: Denkschr. Akad. Wiss. Wien Math.-Nat. Kl., 65, 131, 1898.

Wilson, J. T.: Transform faults, oceanic ridges and magnetic anomalies southwest of Vancouver Island, Science, 150, 482–485, https://doi.org/10.1126/science.150.3695.482, 1965.